Hyperfine Interactions at the Final Positions of $^{56}Fe(n,\gamma)^{57}Fe$ Recoil Nuclei in bcc Iron-Aluminum Alloys*

GORDON CZJZEK
Oak Ridge National Laboratory, Oak Ridge, Tennessee 37830

AND

WOLFRAM G. BERGER
Institut für Angewandte Kernphysik, Kernforschungszentrum Karlsruhe, Karlsruhe, Germany

(Received 26 September 1969)

The results of Mössbauer-effect measurements with 14.4-keV γ rays of ^{57}Fe emitted after thermal-neutron capture by ^{56}Fe in iron-aluminum alloys ($\sim$25 to $\sim$50 at. % Al) are reported. High-energy γ rays emitted in transitions from the capture level at 7.6 MeV to the lowest excited state at 14.4 keV impart recoil energies up to 549 eV to the ^{57}Fe nuclei. Thus the Mössbauer γ rays are emitted by nuclei which have been displaced from their lattice sites. The hyperfine spectra deviate significantly from the spectra obtained with a Cu: ^{57}Co source and the alloy specimens as absorbers. The fraction of ^{57}Fe recoil atoms that come to rest at lattice sites, the number of point defects, and the distribution of iron and aluminum atoms in the immediate neighborhood of their final positions are estimated with a simple collision model. Preliminary estimates of the influence of point defects on hyperfine fields are deduced from the experimental data in conjunction with the model results.

I. INTRODUCTION

IN the past ten years, many theoretical investigations were devoted to the fate of primary recoil atoms and their surroundings in crystalline solids.[1–8] The possibilities for comparison with experimental data are limited, particularly in metals where properties specific to certain defects can hardly be measured directly as in ionic solids by color-center spectroscopy. The relatively young technique of on-line Mössbauer spectroscopy with γ rays originating from the deexcitation of nuclei subsequent to a nuclear reaction[9–15] provides a new source for experimental information on certain aspects of this problem area.

The processes underlying these experiments can be described by a three-step scheme:

(a) The reaction (for example, Coulomb excitation, neutron capture, or deuteron stripping) leads to an excited state of the Mössbauer nucleus. During the reaction itself or in the deexcitation from high-energy states, kinetic energy ($\sim 10^2$–$\sim 10^7$ eV, well above the displacement threshold) is imparted to the nucleus which leaves its lattice site.

(b) The moving nucleus gradually loses its energy to electronic excitations and by transfer of kinetic energy to lattice atoms in collisions, thus creating defects, until it comes to rest somewhere in the lattice. The duration of this process depends on the initial kinetic energy. It is in all cases estimated to be shorter than 10^{-12} seconds.

(c) The low-energy Mössbauer level is populated either directly in the reaction or by cascading transitions from high-energy levels. Its mean lifetime is generally in the range 10^{-9}–10^{-7} sec, some orders of magnitude longer than the duration of the slowing-down process described in paragraph (b). The energy spectrum of the recoil-free emitted γ rays, determined by the time average of the hyperfine interactions over the lifetime of the excited state, is therefore characterized by the environment of the Mössbauer nucleus at the location where it comes to rest. Thermal rearrangements occur in this short time only at high temperatures ($\gtrsim$300°K for typical activation energies of defect migration).

The theoretical investigations[2,5–7] led to the prediction that in pure metals the majority of the recoil nuclei would come to rest at lattice sites, and that frequently vacancies would be found near these sites. The hyperfine spectra obtained in on-line experiments with pure metal targets[9–15] were within the error limits equal to those of nuclei embedded in undisturbed absorbers of the same material. These results definitely

* Research sponsored partly by the U. S. Atomic Energy Commission under contract with the Union Carbide Corporation.

[1] D. K. Holmes and G. Leibfried, J. Appl. Phys. **31**, 1046 (1960).
[2] J. B. Gibson, A. N. Goland, M. Milgram, and G. H. Vineyard, Phys. Rev. **120**, 1229 (1960).
[3] C. Lehmann, Nukleonik **3**, 1 (1961).
[4] M. T. Robinson and O. S. Oen, Phys. Rev. **132**, 2385 (1963).
[5] C. Erginsoy, G. H. Vineyard, and A. Englert, Phys. Rev. **133**, A595 (1964).
[6] C. Erginsoy, G. H. Vineyard, and A. Shimizu, Phys. Rev. **139**, A118 (1965).
[7] P. H. Dederichs, C. Lehmann, and H. Wegener, Phys. Status Solidi **8**, 213 (1965).
[8] J. R. Beeler, Jr., Phys. Rev. **150**, 470 (1966).
[9] S. L. Ruby and R. E. Holland, Phys. Rev. Letters **14**, 591 (1965).
[10] D. W. Hafemeister and E. B. Shera, Phys. Rev. Letters **14**, 593 (1965).
[11] D. Seyboth, F. E. Obenshain, and G. Czjzek, Phys. Rev. Letters **14**, 954 (1965).
[12] Y. K. Lee, P. W. Keaton, Jr., E. T. Ritter, and J. C. Walker, Phys. Rev. Letters **14**, 957 (1965).
[13] J. Christiansen, P. Hindennach, U. Morfeld, E. Recknagel, D. Riegel, and G. Weyer, Nucl. Phys. **A99**, 345 (1967).
[14] W. G. Berger, J. Fink, and F. E. Obenshain, Phys. Letters **25A**, 466 (1967).
[15] G. D. Sprouse, G. M. Kalvius, and S. S. Hanna, Phys. Rev. Letters **18**, 1041 (1967).

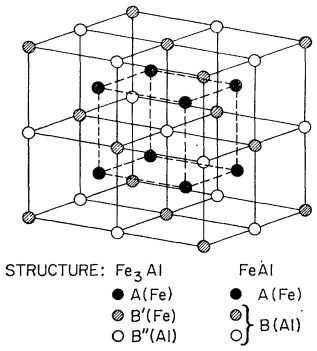

FIG. 1. Sublattice structure of ordered bcc iron-aluminum alloys.

corroborate the first part of the theoretical prediction. The question remains open whether the frequency of nearby vacancies is overestimated by the model calculations, or whether their influence on the hyperfine fields is so weak as to remain undetected.

Here we touch on a large problem area: What are the electronic rearrangements and the resulting changes of hyperfine fields associated with defects? If differences of hyperfine fields from those in undisturbed material are found, and if the nature of the defect causing the difference can be established, the deviation yields quantitative information of relevance to this question.

In the present paper we report results of Mössbauer experiments with 14.4-keV γ rays emitted by ^{57}Fe nuclei after capture of thermal neutrons by ^{56}Fe in ordered iron-aluminum targets ($\sim$25 to $\sim$50 at. % Al). The kinetic energy of the recoil nuclei is less than 550 eV. At this small energy electronic stopping is unimportant. The dominating stopping process is by elastic collisions with lattice atoms.

The hyperfine spectra are significantly different from spectra taken with a Cu:^{57}Co source and with the same alloy specimens as absorbers. Our interpretation of the experimental results is based on simple model calculations in which we extend the method of Ref. 7 with the intention of obtaining quantitative estimates for the numbers of defects and the distribution of iron and aluminum atoms near the final positions of ^{57}Fe recoil nuclei. Preliminary estimates of the influence of point defects on hyperfine fields are deduced from the experimental data in conjunction with the model results.

II. MÖSSBAUER SPECTRA OF ^{57}Fe FOLLOWING NEUTRON CAPTURE IN IRON-ALUMINUM TARGETS

The experiments were performed in a beam of thermal neutrons extracted from the research reactor FR2 at the Kernforschungszentrum Karlsruhe. Details of the experiments have been described elsewhere.[16] In this section we discuss those aspects of the experiments that are of direct consequence to the interpretation: the structure of the alloys, the Mössbauer absorption spectra of the alloys, the distribution of kinetic energies of ^{57}Fe recoil atoms, and the Mössbauer spectra following neutron capture in the alloys.

1. Alloy Targets

Iron-aluminum alloys with less than 54 at.% Al crystallize in the bcc lattice. At room temperature, depending on the aluminum concentration, two ordered structures are the stable phases[17]: In alloys with 25–33 at.% Al this is the DO_3-type structure (Fe_3Al order, see Fig. 1). This phase is ferromagnetic below $\sim$770°K.[18] Between 33 and 52 at.% Al the equilibrium phase has CsCl structure (FeAl order, Fig. 1). This ordered structure is stable up to the melting temperature. Disorder can be introduced by deformation and leads to ferromagnetism.[17] In ordered alloys in this concentration range, no magnetic ordering occurs at temperatures above 20°K.[19]

Both Fe_3Al- and FeAl-type ordering is maintained at concentrations that deviate from stoichiometric composition. In alloys with Fe_3Al order and more than 25 at.% aluminum, surplus aluminum atoms are substituted in sublattice B' (Fig. 1). In alloys with FeAl order, surplus atoms of either kind are substituted in the sublattice which in the ideal compound is occupied by atoms of the other kind. Presumably, substituted atoms are distributed at random in the sublattice. Excess vacancies have not been reported in bcc iron-aluminum alloys.

Specimens of FeAl-type ordering (35.0, 45.0, 48.3, 51.5 at.% Al) were prepared in collaboration with the Institut für Material- und Feskörperforschung.[20] We used powdered target materials which had been annealed for 24 h at 1000°K after crushing. Professor V. Gerold (Max-Planck Institut für Metallforschung, Stuttgart) kindly provided us with very carefully prepared and analyzed Fe_3Al powder (26.75 at.% Al).[21]

2. Mössbauer Absorption Spectra of bcc Iron-Aluminum Alloys

Several investigations on hyperfine interactions of ^{57}Fe in bcc iron-aluminum alloys by Mössbauer spectroscopy have been reported.[22–27] The general conclusion

[16] W. G. Berger, Z. Physik **225**, 139 (1969).

[17] A. Lawley and R. W. Cahn, J. Phys. Chem. Solids **20**, 204 (1961).

[18] L. Pál and T. Tarnoczi, J. Phys. Chem. Solids **23**, 683 (1962).

[19] A. Arrott and H. Sato, Phys. Rev. **114**, 1420 (1959).

[20] H. Schneider and W. Hein, Institut für Material- und Festkörperforschung, Kernforschungszentrum Karlsruhe.

[21] The treatment of this material was similar to that described by G. Lütjering and H. Warlimont, Z. Metallk. **56**, 1 (1965).

[22] C. E. Johnson, M. S. Ridout, and T. E. Cranshaw, Proc. Phys. Soc. (London) **81**, 1079 (1963).

[23] M. B. Stearns, Phys. Rev. **147**, 439 (1966).

[24] L. Cser, J. Ostanevich, and L. Pál, Phys. Status Solidi **20**, 581 (1967); **20**, 591 (1967).

[25] G. K. Wertheim and J. H. Wernick, Acta Met. **15**, 297 (1967).

[26] G. P. Huffman and R. M. Fisher, J. Appl. Phys. **38**, 735 (1967).

[27] M. B. Stearns, Phys. Rev. **168**, 588 (1968).

of these studies was that details of the hyperfine spectra can be described at least approximately if one assumes that individual aluminum atoms in the neighborhood of an iron atom independently affect the hyperfine fields at the nucleus of this atom. The effect of aluminum neighbors decreases with increasing distance from a given iron atom. Over limited concentration regions the effect per aluminum atom in a given coordination shell is approximately constant. A similar influence of neighbor atoms on the hyperfine fields has been observed in other alloy systems.[28–30]

The analysis of all our Mössbauer spectra is based on this model of independent neighbor effects, and we have assumed that it can be extended to point defects in the neighborhood of an iron atom. The influence of aluminum neighbors was deduced from the Mössbauer spectra obtained with a Cu:^{57}Co source and the alloy targets as absorbers.

For specimens with FeAl order the spectrum consisted of a single broadened line. The broadening is attributed to the differences of the environment of iron atoms in the nonstoichiometric alloys. The spectrum is actually a superposition of lines, each with another isomer shift, depending on the number of aluminum neighbors of a resonantly absorbing ^{57}Fe atom:

$$S(N_1, N_2, \ldots N_k, \ldots)=\sum_k N_k I_k. \quad (1)$$

Here N_k is the number of aluminum atoms, I_k is the shift per aluminum atom in the kth coordination shell. For pure iron, $N_k=0$ for all k, and consequently $S=0$. That is, Eq. (1) gives the shift with respect to pure iron. For brevity we will use the term "shift" in this paper in the sense of "shift with respect to iron" unless we state explicitly another reference point.

The measured spectrum was fitted with a single line of Lorentz shape. As we show in Appendix A, the center of this line is in first approximation equal to the weighted average of the centers of the individual lines. The weights are the probabilities $w(N_1,N_2,\ldots N_k,\ldots)$ that an iron atom simultaneously has N_1, N_2, $\ldots N_k$, $\ldots$ Al neighbors in the first, second, $\ldots$, kth, $\ldots$ shell.[31]

$$\langle S\rangle=\sum_{N_1,N_2,\ldots N_k,\ldots} w(N_1, N_2, \ldots N_k, \ldots) \times S(N_1, N_2, \ldots N_k, \ldots). \quad (2)$$

The probabilities $w(N_1,N_2,\ldots N_k,\ldots)$ are determined by the distribution of iron and aluminum atoms in the lattice. With the assumptions about the structure of alloys with FeAl-type order outlined in Sec. (II 1) the average shift, Eq. (2), for a specimen with aluminum concentration C_{Al} can be expressed in terms of two combinations of the I_k:

$$S_1=I_1+3I_4+3I_7+\cdots,$$
$$S_2=I_2+2I_3+\tfrac{4}{3}I_5+I_6+\cdots.$$

The observed shift is

$$\langle S\rangle=[C_{\mathrm{Al}}/(1-C_{\mathrm{Al}})][8S_1+6(1-2C_{\mathrm{Al}})S_2], \quad \text{for } C_{\mathrm{Al}}\leqslant 0.5$$
$$=8S_1+6(2C_{\mathrm{Al}}-1)S_2, \quad \text{for } C_{\mathrm{Al}}\geqslant 0.5. \quad (3)$$

If the shifts due to aluminum neighbors decrease rapidly with increasing distance we can approximately set S_1 equal to I_1, and S_2 equal to I_2. Additional information allowing one to include I_3 and I_4 can, in principle, be derived from the width and asymmetry of the observed spectral line if deviations from the thin-absorber approximation are taken into account. We have not attempted this derivation since we encountered a technical difficulty: The grain size of the alloy powders was not sufficiently small to ensure uniform absorber thickness which is necessary for this kind of analysis. Thus we are working with the approximation of effects due to aluminum neighbors in the first two coordination shells. The values of the two parameters I_1, I_2 are obtained by fitting Eq. (3) to the concentration dependence of the line shift observed at room temperature (Fig. 2, curve 1):

$$I_1=(0.0338\pm 0.0004)\ \mathrm{mm/sec},$$
$$I_2=(0.015\pm 0.004)\ \mathrm{mm/sec}.$$

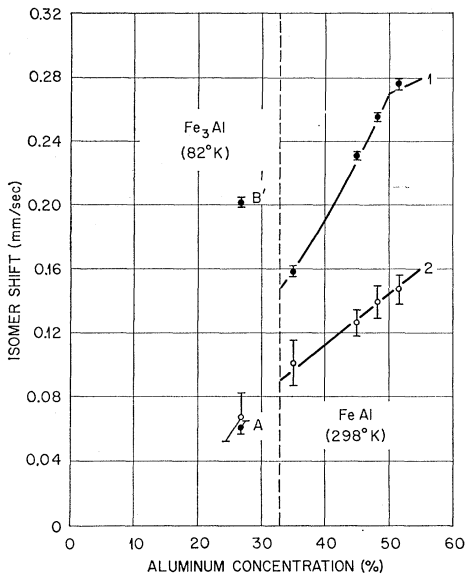

FIG. 2. Isomer shifts in iron-aluminum alloys with respect to iron. ●: absorption spectra; ○: (n,γ)-target spectra. The two points for the Fe_3Al absorber correspond to the indicated lattice sites A and B'. Curve 1 is a fit of the independent-neighbor-effect model to the data. Curve 2 is interpolated between results of model calculations (Sec. III). One parameter has been adjusted such that the measured value for 48.3 at. % Al is reproduced.

[28] V. Jaccarino and L. R. Walker, Phys. Rev. Letters **15**, 258 (1965).
[29] R. L. Streever and G. A. Uriano, Phys. Rev. **149**, 295 (1965).
[30] P. C. Riedi and R. G. Scurlock, Proc. Phys. Soc. (London) **92**, 117 (1967).
[31] This is an approximation applicable for thin absorbers. For thick absorbers the spectrum is not a linear superposition of the individual lines. S. Margulies and J. R. Ehrman, Nucl. Instr. Methods **12**, 131 (1961).

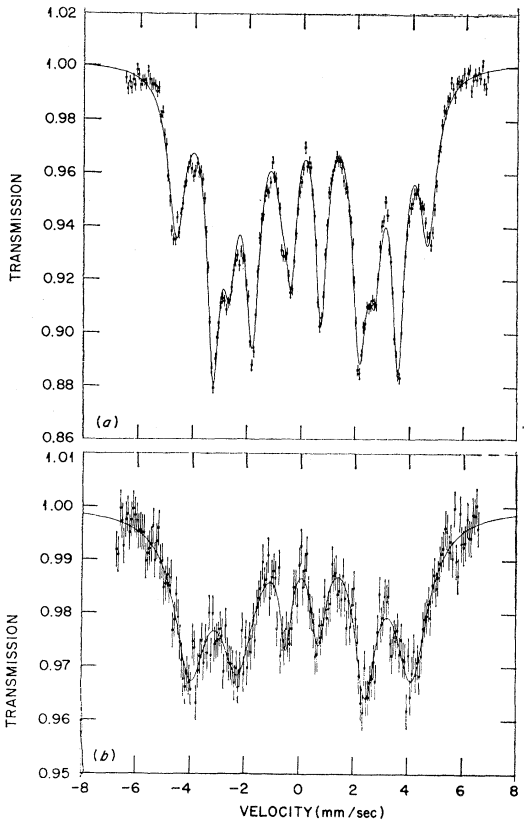

FIG. 3. Mössbauer spectra of Fe_3Al obtained at 298°K. (a) Absorption spectrum with Cu:^{57}Co source, fitted with 12 lines of Lorentz shape; (b) (n,γ)-target spectrum with $Na_4Fe(CN)_6 \cdot 10H_2O$ absorber, fitted with 6 Lorentzian lines. The velocity scale is shifted so that the point $v=0$ coincides with the center of a pure iron Mössbauer spectrum at 298°K.

The Mössbauer absorption spectra of our Fe_3Al specimen at room temperature [Fig. 3(a)] and at 80°K [Fig. 4(a)] agree with those of ^{57}Fe Mössbauer spectra of Fe_3Al reported in the literature.[22,24,27] The spectra are resolved into two sextets corresponding to ^{57}Fe in A sites and B' sites, respectively. We have fitted the experimental data with 12 Lorentzian lines. The number of variable parameters was reduced to 17 by the relations between line positions of a sextet with purely magnetic splitting and isomer shift, and by the assumption that the linewidths and intensities in both sextets are symmetric with respect to their center. This leaves four position parameters, six widths, six intensities, and the background level at infinite velocity.

The temperature dependence of the magnetic hyperfine fields at both A and B' sites deviates significantly from the temperature dependence of the field in pure iron.[27] This fact indicates that aluminum atoms influence the intrinsic magnetic moment of iron atoms and also their coupling to the entire spin system which leads to an additional effect on the average iron moment at nonzero temperature. It cannot be expected that the effect of the atomic distribution in the neighborhood of an iron atom on the spin coupling is describable by the simple neighbor model that we assume for the magnetic hyperfine field. Hence for Fe_3Al we will base our discussion of the results primarily on the data obtained at 80°K where deviations from zero-temperature conditions may be neglected.

As in the alloys with FeAl-type ordering we take into account influences of aluminum atoms in the first and second coordination shell only. Iron atoms in A sites have aluminum neighbors in the first shell, none in the second shell, whereas iron atoms in B' sites have an all aluminum second coordination shell, and only iron atoms as first neighbors. Thus we can obtain the effects of aluminum neighbors in these two shells directly from the splittings and the shifts of the two sextets:

$$I_1 = (0.046 \pm 0.001) \text{ mm/sec},$$
$$I_2 = (0.010 \pm 0.001) \text{ mm/sec},$$
$$\Delta g_1 = (-0.29 \pm 0.01) \text{ mm/sec},$$
$$\Delta g_2 = (-0.027 \pm 0.012) \text{ mm/sec}.$$

The parameters Δg_k are the changes of the ^{57}Fe nuclear ground-state splitting caused by one aluminum atom in the kth shell. The ground-state splitting in pure iron at 80°K is $g_0=4.00$ mm/sec.[32] This splitting is related to the magnetic hyperfine field H by the equation $g_0=0.0118H$ if g_0 is given in mm/sec and H in kOe.

The quantities I_k have the same meaning as defined in the discussion of the spectra of FeAl-structure specimens.

3. Distribution of Kinetic Energies of ^{57}Fe Recoil Nuclei

The kinetic energy of ^{57}Fe nuclei produced by capture of thermal neutrons in ^{56}Fe is due to the recoil of the product nuclei to high-energy γ rays emitted in the deexcitation from the capture level at 7.643 MeV. The distribution of energies is determined by the energies of γ rays emitted, and in cascading transitions it also depends on the lifetime of the intermediate level and on the angular correlation between consecutive γ-ray directions.

The γ-ray spectrum of ^{57}Fe following neutron capture has been investigated by Groshev *et al.*[33] and by Honzatko *et al.*[34] The lifetimes of levels above 706 keV have not been measured. We have used the Weisskopf formula for M1 transitions to estimate these lifetimes. We assume the angular correlation of consecutive γ rays to be isotropic.

---

[32] R. S. Preston, S. S. Hanna, and J. Heberle, Phys. Rev. **128**, 2207 (1962).

[33] L. V. Groshev, A. M. Demidov, G. A. Kotelnikov, and V. N. Lutsenko, Nucl. Phys. **58**, 465 (1964).

[34] J. Honzatko, E. A. Eissa, and K. Konečný, Czech. J. Phys. **B18**, 248 (1968).

The 14.4-keV Mössbauer level in ^{57}Fe is populated in about 47% of the capture events. Only transitions leading to this state are of interest to our work, so we calculate the recoil energy distribution only for these events. In the following context percentages refer to transitions populating the 14.4-keV level.

The transitions of interest can be classified by the following scheme (CL is an abbreviation for the capture level at 7.643 MeV, ML signifies the Mössbauer level at 14.4 keV):

$$\mathrm{CL} \xrightarrow[(E_\gamma=7.629\ MeV)]{} \mathrm{ML} \quad \text{(direct transitions)} \quad (48\%).$$

The recoil energy is $R=E_\gamma^2/2mc^2=549$ eV.

$$\mathrm{CL} \xrightarrow[(E_\gamma=7.277\ MeV)]{} 366\ \mathrm{keV} \begin{cases} \nearrow 137\ \mathrm{keV} \rightarrow \mathrm{ML} \\ \searrow \mathrm{ML} \end{cases} \quad (10\%).$$

The lifetime of the level at 366 keV is 1.1×10^{-11} sec.[35] With great probability the second γ ray is emitted after the nucleus has come to rest. The recoil energy for the low-energy transitions is less than 1 eV, well below the displacement threshold. We assume for this cascade a single recoil energy of 500 eV corresponding to the high-energy transition.

Most of the remaining cascades can be described by one of the following two schemes:

$$\mathrm{CL} \rightarrow \mathrm{IL} \rightarrow \mathrm{ML}$$

$$\mathrm{CL} \rightarrow \mathrm{IL} \rightarrow 366\ \mathrm{keV} \begin{cases} \nearrow 137\ \mathrm{keV} \rightarrow \mathrm{ML} \\ \searrow \mathrm{ML}. \end{cases}$$

IL is an intermediate level in the range ~1 MeV to ~6 MeV. We analyze both schemes in the same way, neglecting contributions from low-energy transitions ($E_\gamma \leqslant 352$ eV) for the reason given in the previous case. For the consecutive high-energy γ pairs we assume that the second emission event occurs before the nucleus, which has recoiled in the first γ emission, has suffered a collision. This assumption is questionable for intermediate levels at ~1 MeV since the estimated lifetime is about $(3\text{ to }5)\times10^{-14}$ sec. The fraction of cases involved is very small, and the recoil energy distribution is not affected strongly. For the pairs of γ rays with isotropic angular correlation, the distribution of recoil energies is constant between the energies $(E_{\gamma_1}-E_{\gamma_2})^2/2mc^2$ and $(E_{\gamma_1}+E_{\gamma_2})^2/2mc^2$, zero outside this range.

For about 5% of the capture events, the cascades are not completely determined and could be more complicated. We have treated these cases by assuming a direct transition from the intermediate level to a low-energy level, neglecting possible contributions from a third energetic γ ray.

[35] G. D. Sprouse and S. S. Hanna, in *Hyperfine Structure and Nuclear Radiations*, edited by E. Matthias and D. A. Shirley (North-Holland Publishing Co., Amsterdam, 1968), p. 761.

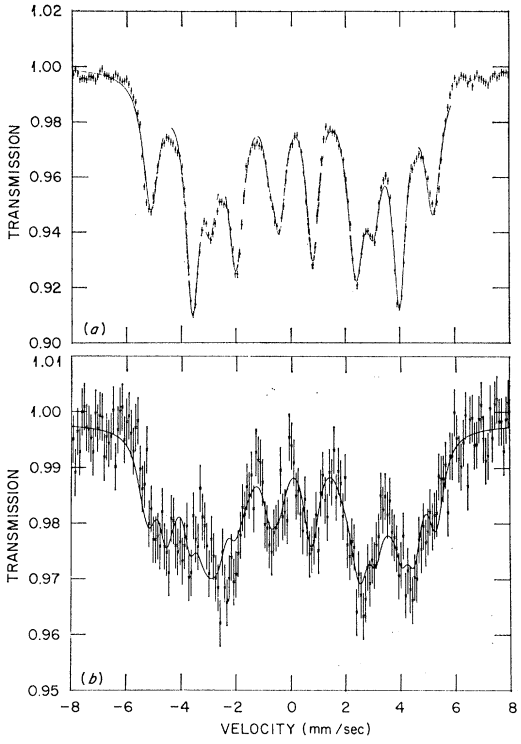

FIG. 4. Mössbauer spectra of Fe_3Al obtained at 82°K. (a) Absorption spectrum, fitted with 12 Lorentzian lines; (b) (n,γ)-target spectrum. The continuous curve is derived from model calculations (Sec. III). The velocity scale is shifted so that the point $v=0$ coincides with the center of a pure iron Mössbauer spectrum at 82°K.

The distribution of kinetic energies of ^{57}Fe recoil nuclei, $P_0(E)$, derived from the γ spectra of Refs. 33 and 34 with the assumptions described in this section is displayed in Fig. 5.

4. Mössbauer Spectra Following Neutron Capture

The Mössbauer spectra obtained with alloys with FeAl order as targets in the neutron beam and a

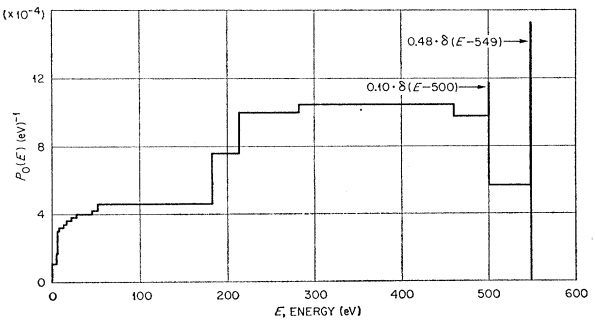

FIG. 5. Distribution of recoil energies of ^{57}Fe nuclei due to emission of high-energy γ rays in deexcitation from the capture level at 7.643 MeV. Only transitions populating the 14.4-keV level are taken into account.

TABLE I. Parameters of (n,γ) Mössbauer spectra in Fe_3Al: $\bar{g}$ is the average value of the ground-state splitting, $\bar{S}$ is the average shift, $M_2^{(a)}$ is the second moment of the magnetic field distribution, a measures the correlation between shifts and fields, and γ is a constant width parameter.

Temperature (°K)	$\bar{g}$ (mm/sec)	$\bar{S}$ (mm/sec)	$M_2^{(a)}$ (mm/sec)^2	a	γ (mm/sec)
82	3.16±0.02	0.067±0.015	0.18±0.02	−0.11±0.04	0.6±0.1
298	2.95±0.02	0.081±0.017	0.10±0.05	−0.1 ±0.2	0.8±0.3

$Na_4Fe(CN)_6\cdot 10H_2O$ absorber (1 mg/cm^2 ^{57}Fe) consisted of a single line similar to those with a Cu:^{57}Co source and these alloy specimens as absorbers. The analysis was again done by fitting a line of Lorentzian shape. The position of the line for an alloy target of any aluminum concentration was significantly different from the position of the absorber line of the same alloy if both positions were measured with respect to the same reference point.

When the emission line is shifted with respect to the absorption line in the same specimen, self-absorption in the target is not symmetric. This leads to a shift between the center of the *emission* line and the center of the *observed* line. In Appendix B we describe the method by which we have estimated this shift for our target spectra.

In Fig. 2 we display the shifts (with respect to iron) of the *emission* lines from the alloy targets with FeAl order. Comparison with the shifts of the absorption lines, also shown in Fig. 2, clearly shows that the average final position of the ^{57}Fe recoil atoms is different from the average position of an iron atom in the lattice.

The same conclusion can be drawn from a comparison of the (n,γ) Mössbauer spectra in the alloy target with Fe_3Al structure, Figs. 3(b) and 4(b), with the absorption spectra Figs. 3(a) and 4(a). Only six resonance lines are resolved. The maximum intensity in the outermost lines occurs at velocities where the effect is small in the absorption spectrum. This intensity must originate from sites not normally occupied by iron atoms in this material.

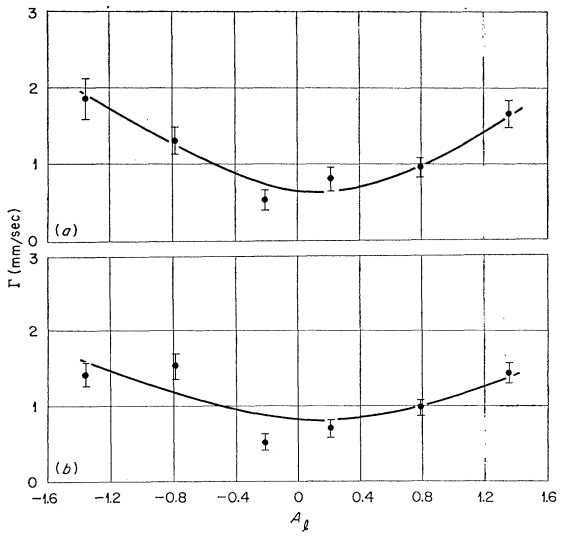

FIG. 6. Widths of Lorentz-shape lines fitted to (n,γ)-target spectra of Fe_3Al. (a) 82°K; (b) 298°K. The hyperbolas are least-squares fits of Eq. (4) to the measured values.

The continuous curve in Fig. 3(b) is obtained by fitting six lines of Lorentz shape to the experimental data. Also the low-temperature spectrum was fitted in this way. We have not imposed any constraints on the fit parameters (six intensities, six positions, six widths, background intensity at infinite velocity). From the positions of the line centers we deduce the values of the average magnetic field (expressed in terms of the ground-state splitting $\bar{g}$) and the average shift $\bar{S}$ listed in Table I. The average quadrupole interaction is zero within error limits, both at 82°K and at room temperature.

We have also analyzed the linewidths of these spectra applying the approach described in Appendix A. We assume that the width Γ_l of the lth line can be represented by the expression

$$\Gamma_l^2=\gamma^2+8A_l^2M_2^{(a)}.$$

Here γ is a constant width, $M_2^{(a)}$ is the second moment of the magnetic field distribution. The A_l are constant coefficients which describe the dependence of the position of the lth line on the magnetic field. If we express the field in terms of the ground-state splitting g, the values of the coefficients A_l are[32]

$$\begin{Bmatrix}A_1\\A_6\end{Bmatrix}=\mp 1.358,\quad \begin{Bmatrix}A_2\\A_5\end{Bmatrix}=\mp 0.786,\quad \begin{Bmatrix}A_3\\A_4\end{Bmatrix}=\mp 0.214.$$

The spectra, especially that taken at 82°K, appear asymmetric. The asymmetry can be caused by a correlation between deviations of isomer shifts and magnetic fields from the average values. We account for the correlation by setting

$$\Gamma_l^2=\gamma^2+8(a+A_l)^2M_2^{(a)}. \tag{4}$$

The parameter a is a measure of the correlation between shifts and fields. The width γ is not necessarily equal to the intrinsic linewidth. It includes broadening due to distributions of shifts and electric field gradients which are not correlated with the magnetic field.

The parameters $M_2^{(a)}$, a, and γ were determined by fitting Eq. (4) to the linewidths derived from the target spectra. The resulting values are given in Table I. The quality of the fit, shown in Fig. 6 [A_l can be regarded as a continuous parameter, proportional to velocity—Eq. (4) then describes a hyperbola in the Γ_l—A_l plane], is satisfactory at 82°K, not so at room temperature.

The discrepancy at room temperature may be due to experimental uncertainty. A physical origin could be a correlation between quadrupole interactions and

TABLE II. Average aluminum concentration α in the neighborhood of the final positions of ^{57}Fe recoil atoms. The average aluminum concentration of the alloy samples is C_{Al}.

Structure	Temperature (°K)	C_{Al}	⟨α derived from⟩ $\bar{S}$	⟨Δg⟩$_{Av}$	⟨α/C_{Al} from⟩ $\bar{S}$	⟨Δg⟩$_{Av}$
Fe_3Al	82	0.2675	0.16±0.03	0.33±0.02	0.60±0.12	1.23±0.08
	298	0.2675	0.20±0.04	0.32±0.02	0.75±0.15	1.20±0.08
FeAl	298	0.35	0.28±0.03	···	0.80±0.08	···
	298	0.45	0.35±0.03	···	0.78±0.08	···
	298	0.483	0.38±0.04	···	0.79±0.08	···
	298	0.515	0.41±0.04	···	0.80±0.08	···

magnetic fields. Such a correlation will occur if asymmetric defects (double vacancies, split interstitials) gain energy by aligning along a preferential direction with respect to the local magnetic field. If reorientation requires thermal activation, the alignment may be suppressed at 82°K, but at room temperature the reorientation may take place in a time shorter than 1.4×10^{-7} sec, the mean lifetime of the 14.4-keV level of ^{57}Fe.

Comparing the average magnetic field and shift of the (n,γ) Mössbauer spectra with the effects of aluminum neighbors deduced from the absorption spectra of the alloys, we can estimate the average aluminum concentration α in the neighborhood of the recoil atom at its final site provided defects do not contribute shifts or magnetic effects:

$$\bar{S}=\alpha(8I_1+6I_2)=0.362\alpha, \quad \text{for FeAl structure}$$
$$=0.428\alpha, \quad \text{for } Fe_3Al \text{ structure},$$
$$\langle\Delta g\rangle_{av}=\bar{g}-g_0=\alpha(8\Delta g_1+6\Delta g_2)$$
$$=-2.536\alpha, \quad \text{for } Fe_3Al \text{ at } 82°K$$
$$=-3.137\alpha, \quad \text{for } Fe_3Al \text{ at } 298°K,$$

where g_0 is the ground-state splitting of ^{57}Fe in pure iron ($g_0=4.00$ mm/sec at 82°K, $g_0=3.92$ mm/sec at 298°K).[32]

The values of α derived in this way and the ratios α/C_{Al} are listed in Table II. If all ^{57}Fe recoil atoms come to rest at lattice positions irrespective of previous occupancy, and without disturbances in the neighborhood, the ratio α/C_{Al} should be equal to unity. The isomer shifts of the (n,γ) Mössbauer spectra give for all concentrations nearly the same relative aluminum depletion of 20% compared to the average concentration. The result for Fe_3Al at 82°K points to an environment even poorer in aluminum, but the experimental uncertainty of this result is large.

However, the change of the magnetic field in Fe_3Al is about 20% larger than expected for a neighborhood with average aluminum concentration.

This discrepancy between field changes and isomer shift would be explained by the assumption that the field decreases more rapidly than linearly with the number of aluminum neighbors. It has been shown that such a deviation from linearity is likely.[26] But it seems to occur only when more than four aluminum atoms are in the first coordination shell of an iron atom. And then the field goes almost immediately to zero. A frequent occurrence of more than four aluminum atoms in the first coordination shell of the recoil atoms in Fe_3Al disagrees with our isomer-shift data, and the (n,γ) Mössbauer spectra of Fe_3Al definitely do not show any evidence of an unsplit line.

We believe that the apparent discrepancy between the average isomer shift and the average magnetic field is caused by point defects in the vicinity of the recoil atoms.

The hypothesis of defect influences on the hyperfine spectrum can be tested experimentally by taking (n,γ) Mössbauer spectra at various temperatures. At sufficiently high temperature all defects become mobile. The average frequency ν_j at which a defect jumps from one site to another can be estimated roughly by the relation $\nu_j\approx\nu_0\exp(-G/kT)$.[36] In this expression $\nu_0\approx10^{13}$ sec^{-1} is an effective frequency associated with vibration of the defect, and G is the free energy needed to carry the defect from an initial equilibrium position to a saddle point. Changes of the hyperfine spectrum can be expected when $\nu_j>n/\tau\approx n\times10^7$ sec^{-1}. For a vacancy or an interstitial in the neighborhood $n\sim2$–3 should suffice to reduce the influence on the hyperfine spectrum. If the emitting atom itself is an interstitial, the number n of jumps during the lifetime of the 14.4-keV level must be large enough to lead to annihilation with a vacancy unless diffusion occurs by the interstitialcy mechanism.

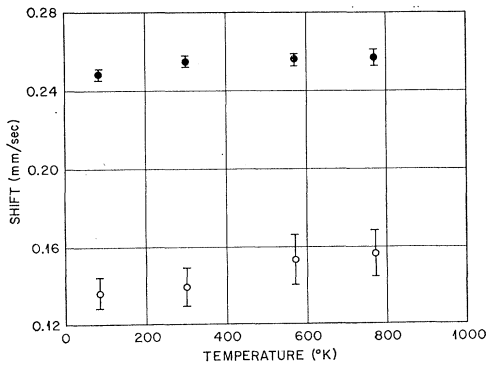

FIG. 7. Temperature dependence of the shift (with respect to iron) obtained with an FeAl-structure alloy with 48.3 at. % aluminum. ● absorption spectra; ○ (n,γ)-target spectra.

[36] A. C. Damask and G. J. Dienes, *Point Defects in Metals* (Gordon and Breach, Science Publishers, Inc., New York, 1963).

We have taken Mössbauer spectra with a specimen of FeAl structure (0.483 at.% Al) at four different temperatures between 80 and 770°K. The shifts both of absorber and of target resonance lines (with respect to iron) are shown in Fig. 7. There is no drastic temperature dependence of the shift. The small change of the absorber shifts is presumably due to a second-order Doppler shift. In the framework of a Debye model the observed change can be expressed by the statement that the Debye temperature of the alloy is (40 ± 10)°K higher than the Debye temperature of pure iron. The temperature dependence of the target shifts could also be interpreted as second-order Doppler shift, but the increase in Debye temperature, $\Delta\Theta = (100\pm30)$°K, seems very high.

If the change of the shifts between room temperature and 570°K can be interpreted as caused by defect migration (and we see no other plausible explanation), it leads to an activation energy $Q\sim(0.4\pm0.1)$ eV. This is close to the energy expected for interstitial migration.[36] The change of the shift in this temperature region is only about 0.02 mm/sec, less than 20% of the total shift between absorber line and target line. We can conclude that either the number of interstitials or the shift caused by interstitials is small.

The highest temperature of our experiments, $T=770$°K, corresponds to an activation energy $Q\sim0.8$ eV. Since the migration energy for vacancies is near 1 eV,[35] we can not expect to see changes due to the motion of vacancies. Unfortunately, experiments in the neutron beam at higher temperatures meet severe technical difficulties, and we were not able to reach the temperature region where we could expect vacancies to be mobile.

III. MODEL CALCULATIONS ON FINAL POSITIONS OF ^{57}Fe RECOIL ATOMS IN IRON AND IN IRON-ALUMINUM ALLOYS

For an interpretation of the Mössbauer spectra obtained with neutron-capture targets we want to estimate the nature of the final positions of the recoil atoms emitting 14.4-keV γ rays.

The principal questions are: How many recoil atoms come to rest in lattice sites? How many are stopped in interstitial positions? How many vacancies and interstitials are likely to be found in the neighborhood of atoms ending in lattice sites? And for the alloys we need to know the distribution of iron and aluminum atoms in the vicinity of the replacement site.

Numerical calculations like those of the Brookhaven group[2,5,6] give, in principle, the most detailed answers to all these questions. But many calculations of individual recoil atom histories would be needed to provide sufficient statistical material to deduce quantitatively the defect distribution near the final position of primary recoil atoms. Such information could not be extracted from the publications of Erginsoy and co-workers since the authors were not aiming at these particular results, and their work refers only to pure metals. Detailed calculations on recoil atom positions in alloys have not been published.

We have now attacked the problems with a method similar to that used by Dederichs *et al.*,[7] extending their approach to include those local-collision events which are the most important ones for the production of defects near the final positions of recoil atoms.

The main objective of the present work was to test the principle of the method and to obtain a guideline for the interpretation of the experimental data. Therefore we have used the approximation of elastic collisions between hard-sphere atoms which greatly simplified the calculations. Also, detailed information is not available on the parameters needed for a more elaborate investigation of the collision processes in iron-aluminum alloys, and only for these materials do our Mössbauer data give a positive indication of defect influences. But the model is not confined to this approximation, and it should be improved by a more realistic assumption for the interaction between energetic atoms in a solid in order to obtain a better quantitative estimate of the defect distribution near the final position of recoil atoms in alloys.

1. Basic Features of Model

Collisions between a moving atom of kinetic energy E and a lattice atom, assumed at rest, can be characterized by the distribution $f(E_T,E)$ of transferred energies E_T, or alternatively by the distribution $g(\epsilon,E)$ of retained energies ϵ. The functions f and g depend on the interaction between the atoms, on energy losses in inelastic collisions, and on the initial directional distribution of the moving atoms. The directional distribution can be expressed in terms of the distribution $p(b)$ of impact parameters b.

In our model we distinguish between homogeneous collision events and local collision processes. For homogeneous events we assume a constant particle current through any surface element in the solid. The corresponding distribution of impact parameters is

$$p_h(b)\,db=2\pi b\,db. \tag{5}$$

This assumption is appropriate for collision events whose localization is not specified. We will occasionally use the phrase "somewhere in the lattice" to characterize collisions of this kind.

In the alloys, collisions occur with iron or with aluminum atoms. We assume that the probability q_K ($K=1$ for iron, $K=2$ for aluminum) for a collision with one or the other atomic species "somewhere in the lattice" is given by

$$q_K=C_K\sigma_K/(C_1\sigma_1+C_2\sigma_2), \tag{6}$$

where C_K is the concentration of K-type atoms, σ_K is

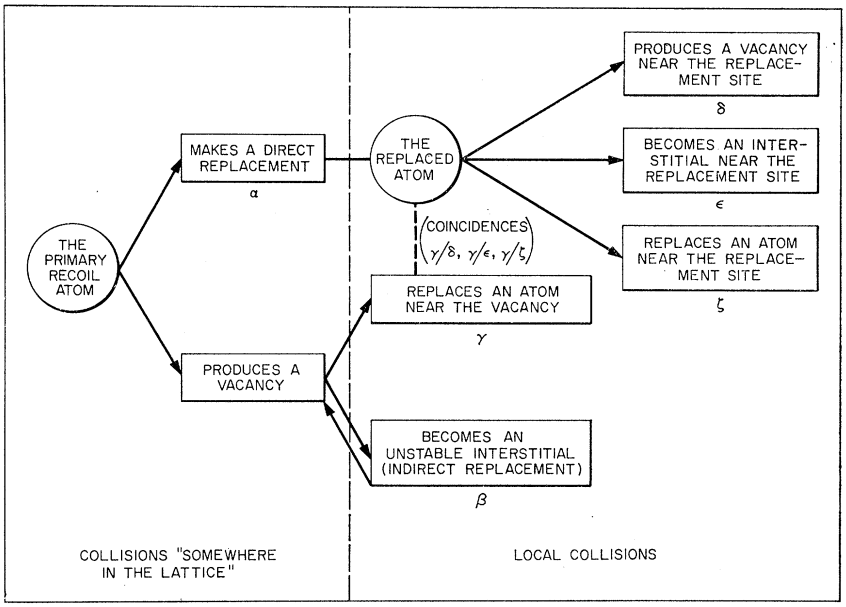

FIG. 8. Schematic flow chart of the collision processes whose probabilities are calculated.

the total cross section for a collision of a moving iron atom with a lattice atom of type K. This expression, exact for a random solid, is a good approximation if the flight path between collisions exceeds one or two lattice constants.

The second class of processes are collisions occurring in the neighborhood of a specific lattice site, the location of a foregoing collision. For local collisions of the atom originally occupying the site and knocked out in the first collision we can assume an isotropic particle current emerging from the center of the site. The distribution of impact parameters in a collision with a lattice atom at distance A from the site is then

$$p_1(b)\,db = b\,db/[2A\times(A^2-b^2)^{1/2}]. \qquad (7)$$

We use the same formula for treating local collisions of the recoil atom after it has knocked an atom out of a lattice site and thereby has produced a vacancy. This approximation allows the general treatment of local processes.

The probability of the following collision events has been calculated:

(α) Replacement collisions as defined in Ref. 7; we introduce the notation "direct replacements" to distinguish these events from indirect replacements.

(β) Indirect replacements: the recoil atom produces a vacancy in a collision with a lattice atom and is then stopped in a subsequent collision with atoms near the vacant site, thus becoming an unstable interstitial which reunites with the vacancy in a short time, presumably less than 10^{-9} sec.[37]

[37] An inspection of the pictures published by C. Erginsoy *et al.* (Ref. 6) shows that this process might contribute significantly to the number of recoil atoms ending at lattice sites.

(γ) The recoil atom makes a replacement collision in the neighborhood of a vacancy which it has produced in the foregoing collision.

(δ) The recoil atom replaces a lattice atom, and the replaced atom produces a vacancy in a collision with a neighbor.

(ϵ) The replaced atom is stopped to become an interstitial in the neighborhood of the recoil atom.

(ζ) The replaced atom makes a replacement collision near the recoil atom. This process is of interest only when it leads to an exchange of two atoms of different kind in alloys.

The collision sequences of these processes are shown schematically in form of a flow diagram in Fig. 8.

Those recoil atoms that do not replace a lattice atom by process α or β are considered ending in interstitial sites.

Other possibilities for generation of defects near the final position of the recoil atom, by atoms which have been knocked out of their lattice site, but are not replaced by the recoil atom, are neglected. Simple considerations of the solid angles involved show that the probability of such uncorrelated defect production near the final position of the recoil atom is at least an order of magnitude smaller than the probability for defect generation by the correlated events listed above. This statement also holds for the atom removed from the vacancy site in process γ, particularly for the production of defects in the first coordination shell of the replacement site.

We also neglect the possiblity of multiple collisions in the immediate neighborhood of the location of replacement.

2. Quantitative Formulation

In the case of elastic collisions between hard spheres the transfer functions for events "somewhere in the lattice," characterized by the subscript h, and local events, subscript l, have the form

$$f_h(E_T,E)=1/rE, \quad \text{for } 0<E_T<rE$$
$$=0, \quad \text{for } rE<E_T, \tag{8}$$

$$g_h(\epsilon,E)=0, \quad \text{for } 0<\epsilon<(1-r)E$$
$$=1/rE, \quad \text{for } (1-r)E<\epsilon<E$$
$$=0, \quad \text{for } E<\epsilon, \tag{9}$$

$$f_l(E_T,E)=\tfrac{1}{4}S[(1-S)r^2E^2+rSEE_T]^{-1/2}, \quad \text{for } 0<E_T<rE$$
$$=0, \quad \text{for } rE<E_T, \tag{10}$$

$$g_l(\epsilon,E)=0, \quad \text{for } 0<\epsilon<(-r)E$$
$$=\tfrac{1}{4}S[(1+Sr-Sr^2)E^2-rSE\epsilon]^{-1/2}, \quad \text{for } (1-r)E<\epsilon<E$$
$$=0, \quad \text{for } E<\epsilon, \tag{11}$$

with

$$r=4m_1m_2/(m_1+m_2)^2, \quad S=[(R_1+R_2)/A]^2.$$

The quantities m_i are the masses, R_i are the hard-sphere radii of the colliding atoms; A is the distance between the center of the site from which the moving atoms emerge and the site of the lattice atom involved in the collision.

The transfer functions for collisions "somewhere in the lattice" are normalized to 1:

$$\int_0^{rE} f_h(E_T,E)dE_T=\int_{(1-r)E}^{rE} g_h(\epsilon,E)d\epsilon=1.$$

This normalization is equivalent to assuming a crystal of infinite size where a collision certainly will occur, a condition appropriate to describe the situation in our experiments. The corresponding integral over the local transfer functions gives the total probability for a collision with an atom at distance A from the distinguished site.

The hard-sphere radii R_i were set equal to the distance of closest approach under a screened Coulomb interaction between the atoms.[38] We introduce the notation $R=R_1+R_2$, $a=\lambda a_0/(Z_1^{2/3}+Z_2^{2/3})^{1/2}$ with the Bohr radius $a_0=0.529\times10^{-8}$ cm, the nuclear charge Z_i of atom i (we use $i=1$ to designate the moving atom, $i=2$ for the lattice atom). The parameter λ is an adjustable factor. $R(E)$ is obtained from the equation

$$\frac{Z_1Z_2e^2}{R}\exp\left(-\frac{R}{a}\right)=\frac{m_2}{m_1+m_2}E.$$

In the calculations we have used $\lambda=1.7$. With this choice of λ the iron-iron potential is very close to that used in Refs. 5 and 6 in that region where the potential used by these authors is repulsive.

Another approximation of our calculations was the assumption of a single threshold energy E_d which we have chosen to be 25 eV. Again the introduction of a more realistic assumption into the model was not prevented by basic difficulties but rather by the scarcity of information regarding the alloys.

We also had to quantify the condition that the atom is stopped to become an interstitial. We have done this by assuming that the atom is stopped when its energy is smaller than an interstitial threshold energy E_i. In the calculations we have set $E_i=E_d=25$ eV.

The probabilities of local processes were calculated for the first and second coordination shells in the cases of local replacements (processes γ and ζ) and vacancy production (process δ). For the local generation of interstitials (processes β and ϵ) we have also included collisions with third-shell neighbors. This corresponds approximately to the region of instability of an interstitial near a vacancy in bcc iron.[5] The tails of this region extending in the (111) direction were neglected. Sites there can only be reached in multiple-collision processes and the probability for such events should be small.

The probability that an atom of energy E in a collision with a lattice atom will make a replacement collision, produce a vacancy, or will be stopped under the interstitial threshold is determined by integrating one of the functions (8)–(11) over the appropriate range of E_T or ϵ. The limiting values are:

for a replacement collision

$$E_d<E_T<rE \quad \text{and} \quad (1-r)E<\epsilon<E_d; \tag{12a}$$

for production of a vacancy

$$E_d<E_T<rE \quad \text{and} \quad \mathrm{Max}(E_d,(1-r)E)<\epsilon<E; \tag{12b}$$

for stopping below the interstitial threshold

$$0<E_T<E_d \quad \text{and} \quad (1-r)E<\epsilon<E_i. \tag{12c}$$

The limits both for E_T and for ϵ have to be taken into account in each case. The more restrictive one at a given energy E determines the limits of integration.

In the remaining part of this section we will describe in detail our calculation of the probabilities of processes α and β. This will exemplify the method.

The calculations are carried out for an ensemble of recoil atoms with the energy distribution given in Sec. II 3 which now has to be slightly modified. All atoms with recoil energy $E<E_d$ do not leave their lattice site. In addition, some atoms with recoil energy E in the range $E_d<E<E_d+E_i$ are stopped in collisions with neighboring atoms and return to their original site. The probability of this event is calculated in the same way as the probability for process β to be described below. The atoms which are stopped are re-

[38] F. Seitz and J. S. Koehler, in *Solid State Physics* (Academic Press Inc., New York, 1956) Vol. 2, p. 307.

moved from the ensemble and after this modification we obtain the energy distribution $P_0(E_0)$ of freely moving recoil atoms.

This distribution is now changed by collisions of the recoil atoms with lattice atoms. In a monatomic solid the energy distribution $P_1^0(E_1)$ following the first collision of all atoms from the ensemble is given by[7]

$$P_1^0(E_1)=\int_{E_0=E_1}^{E_0=E_{\max}} g_h(E_1,E_0)P_0(E_0)dE_0. \quad (13)$$

In iron-aluminum alloys, collisions may occur with iron or aluminum atoms. The relative probability for collisions with one or the other atomic species is by assumption given by the expression Eq. (6). The transfer function g_h differs in the two cases via the parameter r. Thus the energy distribution after the first collision in the alloy is, according to our model,

$$P_1^0(E_1)=q_{\mathrm{Fe}}\int_{E_0=E_1}^{E_0=E_{\max}} g_h^{\mathrm{Fe}}(E_1,E_0)P_0(E_0)dE_0 + q_{\mathrm{Al}}\int_{E_0=E_1}^{E_0=\mathrm{Min}(E_{\max},\,E_1/(1-r))} \times g_h^{\mathrm{Al}}(E_1,E_0)P_0(E_0)dE_0.$$

This recursion formula for the energy distribution after the first collision can be generalized immediately to that for the distribution after the nth collision:

$$P_n^0(E_n)=q_{\mathrm{Fe}}\int_{E_{n-1}=E_n}^{E_{n-1}=E_{\max}} g_h^{\mathrm{Fe}}(E_n,E_{n-1})P_{n-1}(E_{n-1})dE_{n-1} + q_{\mathrm{Al}}\int_{E_{n-1}=E_n}^{E_{n-1}=\mathrm{Min}(E_{\max},\,E_n/(1-r))} \times g_h^{\mathrm{Al}}(E_n,E_{n-1})P_{n-1}(E_{n-1})dE_{n-1}. \quad (14)$$

We can now proceed to calculate the fraction R_n of the recoil atoms making a direct replacement (process α) in the nth collision. [With the normalization $\int_0^{E_{\max}} P_0(E)dE=1$, we can also call R_n the probability for a direct replacement in the nth collision. Both expressions will be used.] For comparison with the Mössbauer spectra of iron-aluminum alloys we have to find the distribution of atoms in the neighborhood of the replacement site which depends on the sublattice to which the site belongs. We introduce the probability R^G for a direct replacement at a site belonging to sublattice G (in Fe_3Al G symbolizes A, B', or B''). It is related to the probability for a direct replacement with an iron (R^{Fe}) or aluminum (R^{Al}) atom by the equation $R^G=Q_{\mathrm{Fe}}{}^G R^{\mathrm{Fe}}+Q_{\mathrm{Al}}{}^G R^{\mathrm{Al}}$, where the quantities $Q_k{}^G$ are the fractions of k-type atoms occupying G sites. The probabilities R^k finally are given by the probability that the conditions (12a) are fulfilled after a collision of a recoil atom with a lattice atom of type k:

$$R_n{}^{\mathrm{Fe}}=q_{\mathrm{Fe}}\left(\int_{E_d}^{2E_d} dE_{n-1}\,P_{n-1}(E_{n-1})\int_0^{E_{n-1}-E_d} d\epsilon\, g_h^{\mathrm{Fe}}(\epsilon,E_{n-1})+\int_{2E_d}^{E_{\max}} dE_{n-1}\,P_{n-1}(E_{n-1})\int_0^{E_d} d\epsilon\, g_h^{\mathrm{Fe}}(\epsilon,E_{n-1})\right), \quad (15a)$$

$$R_n{}^{\mathrm{Al}}=q_{\mathrm{Al}}\left(\int_{E_d/r}^{2E_d} dE_{n-1}\,P_{n-1}(E_{n-1})\int_{(1-r)E_{n-1}}^{E_{n-1}-E_d} d\epsilon\, g_h^{\mathrm{Al}}(\epsilon,E_{n-1}) + \int_{2E_d}^{E_d/(1-r)} dE_{n-1}\,P_{n-1}(E_{n-1})\int_{(1-r)E_{n-1}}^{E_d} d\epsilon\, g_h^{\mathrm{Al}}(\epsilon,E_{n-1})\right). \quad (15b)$$

In these equations we have again introduced the subscripts referring to the number of the collision.

The quantities $R_n{}^G$ are now multiplied by the weight factors $w_G(n_1,n_2)$ specifying the likelihood of finding n_j aluminum atoms in the jth coordination shell of a site in sublattice G.

With this step the determination of the fraction of recoil atoms making a direct replacement in the nth collision and their distribution over lattice sites has been completed.

Indirect replacements (process β) occur by a two-step process. At first a vacancy (the site of the replacement) is produced in the nth collision. The distribution $P_V{}^k(\epsilon)$ of retained energies ϵ after a vacancy-generating collision with a k-type atom is

$$P_{V,n}{}^k(\epsilon)=\int_{E_{n-1}=\epsilon+E_d}^{E_{n-1}=\mathrm{Min}(E_{\max},\,\epsilon/(1-r))} \times dE_{n-1}g_h{}^k(\epsilon,E_{n-1})P_{n-1}(E_{n-1}), \quad (E_d<\epsilon<E_{\max}-E_d),$$

$$P_{V,n}{}^k(E)=0, \quad (\epsilon<E_d,\ \epsilon>E_{\max}-E_d).$$

We have to find the probability for an indirect replacement in a given sublattice G for determining the atomic distribution in the neighborhood of the replacement site. The distribution $P_{V,n}{}^G(\epsilon)$ of retained energies ϵ

after production of a vacancy in sublattice G in the nth collision is given by

$$P_{V,n}{}^{G}(\epsilon)=Q_{\mathrm{Fe}}{}^{G}q_{\mathrm{Fe}}P_{V,n}{}^{\mathrm{Fe}}(\epsilon)+Q_{\mathrm{Al}}{}^{G}q_{\mathrm{Al}}P_{V,n}{}^{\mathrm{Al}}(\epsilon). \quad (16)$$

In a second collision with an atom in one of the first three coordination shells of the site of the first collision, the recoil atom must be stopped below the interstitial threshold E_i. This second, local, collision is characterized by the transfer function, Eqs. (10) and (11). The probability $u_k{}^{j}(\epsilon)$ that a recoil atom of energy ϵ is stopped in a collision with one atom of type k in the jth coordination shell is obtained by integrating the transfer function Eq. (10) over the range of transferred energies E_T specified by Eq. (12c):

$$u_{\mathrm{Fe}}{}^{j}(\epsilon)=\int_{E_T=\epsilon-E_i}^{E_T=E_d} dE_T\, f_l{}^{j,\mathrm{Fe}}(E_T,\epsilon), \quad \text{for } E_d<\epsilon<E_d+E_i, \quad (17a)$$

$$u_{\mathrm{Al}}{}^{j}(\epsilon)=\int_{E_T=\epsilon-E_i}^{E_T=r\epsilon} dE_T\, f_l{}^{j,\mathrm{Al}}(E_T,\epsilon), \quad \text{for } E_d<\epsilon<(1/r)E_d$$

$$=\int_{E_T=\epsilon-E_i}^{E_T=E_d} dE\, f_l{}^{j,\mathrm{Al}}(E_T,\epsilon), \quad \text{for } (1/r)E_d<\epsilon<E_d+E_i. \quad (17b)$$

The local-transfer function $f_l{}^{j,k}$ depends on the shell label j via the distance A_j, and on the atomic species via the parameters S and r.

The total stopping probability $u_{n_j}{}^{j}(\epsilon)$ in a shell containing n_j aluminum atoms and (N_j-n_j) iron atoms is the sum over the stopping probabilities at the individual atoms:

$$u_{n_j}{}^{j}(\epsilon)=(N_j-n_j)u_{\mathrm{Fe}}{}^{j}(\epsilon)+n_j u_{\mathrm{Al}}{}^{j}(\epsilon). \quad (18)$$

At this point we have to account for the possibility that atoms in remote coordination shells may be partly or totally hidden behind atoms in closer shells. The fraction of the remote atoms that is covered by closer atoms depends on the energy and the factor λ in the screening radius. For $\lambda=1.7$ about 17% (75%) of the second (third) neighbors' cross section is covered by the cross sections of the first neighbors at the energy $E=25$ eV. We have used an approximate method of handling the problem: Neglecting the energy dependence of the covered fraction of the atoms, we have chosen values of the distance parameters A_j for $j=2, 3$ that were larger than the true distance in the lattice. Since the collision cross section σ for local processes occurs only in the combination σ/A^2, this procedure is equivalent to a reduction of the cross section. The increase of A_j was chosen such as to account approximately for the average covering in the energy region of interest.

With this provision we can add the probabilities for stopping in the first three coordination shells. To complete the calculation we have to integrate the result over ϵ, weighted with the distribution $P_{V,n}{}^{G}(\epsilon)$ of retained energies after the vacancy-producing collision. The atomic distribution in the three coordination shells has to be taken into account, but since we assume that only first and second neighbors contribute to the measured hyperfine interactions, we average over the occupations of the third shell.

Thus, we obtain the fraction $S_n{}^{G}(n_1,n_2)$ of recoil atoms making in the nth collision an indirect replacement at a G site with $n_1(n_2)$ aluminum neighbors in the first (second) coordination shell:

$$S_n{}^{G}(n_1,n_2)=\sum_{j,n_3} w_G(n_1,n_2,n_3) \times\int_{\epsilon=E_d}^{\epsilon=E_d+E1} d\epsilon\, u_{n_j}{}^{j}(\epsilon)P_{V,n}{}^{G}(\epsilon). \quad (19)$$

The total fraction $T_n{}^{G}(n_1,n_2)$ of recoil atoms replacing a lattice atom at a specified site is then

$$T_n{}^{G}(n_1,n_2)=R_n{}^{G}w_G(n_1,n_2)+S_n{}^{G}(n_1,n_2). \quad (20)$$

The atoms making a replacement in the nth collision have to be subtracted from the distribution of atoms moving freely after this collision. For direct replacements this is simply done by cutting off the part of the distribution which is below the displacement threshold E_d. Indirect replacements in the nth collision occur if the energy E_n is in the range $E_d<E_n<E_d+E_i$. The distribution is modified to

$$P_n(E_n)=P_n{}^{0}(E_n) - \sum_{G,j;\, n_1,n_2,n_3} w_G(n_1,n_2,n_3)u_{n_j}{}^{j}(E_n)P_{V,n}{}^{G}(E_n), \quad (E_d<E_n<E_d+E_i)$$

$$=P_n{}^{0}(E_n), \quad (E_d+E_i<E_n). \quad (21)$$

The calculations of the probabilities for the other processes, γ to ζ, are basically similar to the procedure demonstrated for process β, and we feel that the differences in the details do not justify an explicit presentation. But a few general remarks should be added.

In the local processes γ to ζ we consider only direct replacement collisions in conjunction with the generation of a defect. For the fraction of vacancies in the neighborhood, the neglect of indirect replacements is at least partly balanced, or possibly overbalanced, by those events in which the atom which is knocked out of its lattice site in the vacancy-producing collision becomes an unstable interstitial near the vacancy and returns to its original site. In other cases the neglect of indirect replacements should not be very serious. The probability of indirect replacements is found to be about 20–30% of the probability for direct replacements. We do not believe that this neglect exceeds other errors due to approximations introduced in the calculations.

We have in a simple way accounted for the possibility of coincidence of two local processes at one site.

Processes δ, ϵ and ζ are mutually exclusive if we neglect multiple collisions in the immediate neighborhood of a site. Process γ can coincide with any one of the processes δ, ϵ, and ζ.

Let us introduce the quantities $\Gamma_n{}^G(n_1,n_2)$, $\Omega_n{}^G(n_1,n_2)$, and $D_n{}^G(n_1,n_2)$ in analogy to $T_n{}^G(n_1,n_2)$ but Γ referring to the fraction of recoil atoms involved in a process of type γ, Ω to any one of the processes δ, ϵ, ζ, and D to a coincidence process in the nth collision at site $G(n_1,n_2)$. We set $D_n{}^G(n_1,n_2)=F\Gamma_n{}^G(n_1,n_2)\Omega_n{}^G(n_1,n_2)/T_n{}^G(n_1,n_2)$. The factor F in this equation determines the likelihood of a coincidence. For $F=0$ coincidences do not occur. The value $F=1$ is equivalent to the assumption that the processes δ, ϵ, ζ occur with the same probability if the recoil atom replaces a neighbor of a vacancy that it had generated in the foregoing collision as when the replacement collision occurs at some further distance from the site of the previous collision. Values $F>1$ are also possible. We have done our calculations with $F=1$ and some test runs with other values of F. The results do not depend strongly on the choice of F. For the coincidences γ/ϵ we assume that the interstitial atom generated in process ϵ reunites with the vacancy. The total number of defects is thus slightly reduced as F is increased.

3. Results of Model Calculations

The model calculations for pure iron and for alloys with Fe_3Al and FeAl structure outlined in Sec. III 2 were programmed for the IBM 360/91 computer. The computation followed the sequence of collisions for an ensemble of recoil atoms with the given distribution of initial energies, and stopped when less than 0.5% of the original ensemble was still moving freely. This limit was in all cases reached after the ninth or tenth collision.

The gradual depletion of the ensemble and the losses of kinetic energy in the collisions are illustrated in Fig. 9(a) for pure iron. Figure 9(b) shows the fraction of recoil atoms replacing a lattice atom, and in Fig. 9(c) we show those fractions of all atoms ending at a lattice site in a collision that have a vacancy in the first coordination shell, and those having an interstitial in the neighborhood. These figures show results of calculations for pure iron assuming independent occurrence of two processes, that is, with a coincidence factor $F=1$.

The final results of the calculations are summarized in Table III. The general trend is a decrease of the replacement probability and of the frequency of vacancies near the recoil atom and an increase of the number of nearby interstitials with increasing aluminum concentration.

The distribution of the replacement sites over the sublattice shows that within our model the probability for replacements at an iron site is about 1.5 times that for replacements at an aluminum site. The ratio of the probabilities is 1.7 for direct replacements. Consequently, recoil atoms preferentially occupy iron sites,

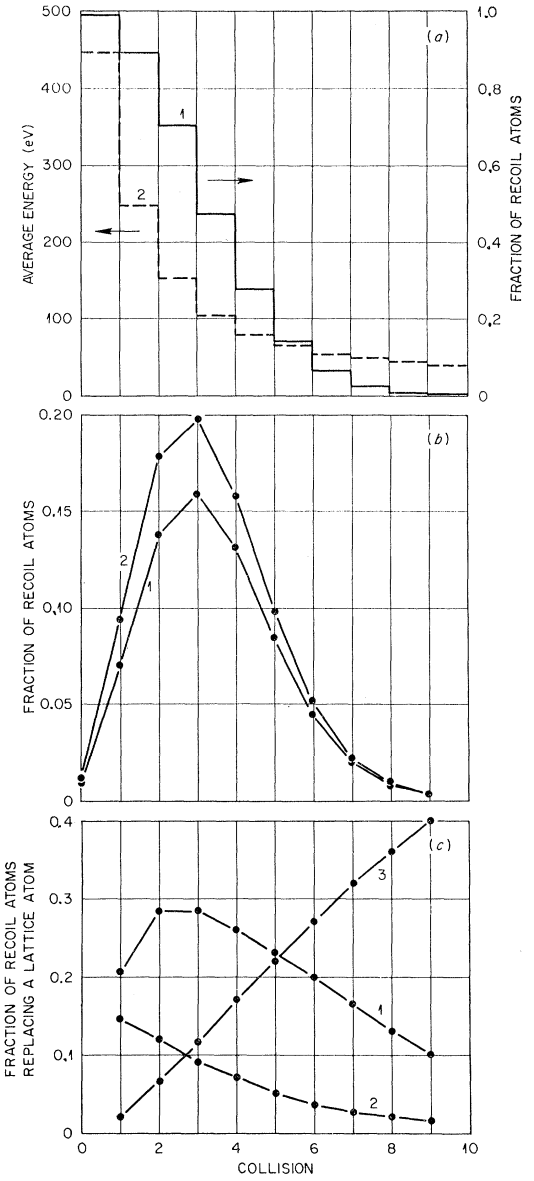

FIG. 9. Details of the model results on the slowing-down process of ^{57}Fe recoil atoms in *pure iron*. In Figs. 9(b) and 9(c) only the points have meaning. The lines are merely optical aids connecting points that mark the same process. (a) Curve 1: Fraction of recoil atoms moving freely after the nth collision. About 1% of the atoms do not leave their original lattice site. Curve 2: Average energy of free-moving recoil atoms. (b) Line 1: Fraction of recoil atoms making a direct replacement in the nth collision. Line 2: Fraction of recoil atoms making a replacement (direct+indirect) in the nth collision. (c) Fraction of recoil atoms replacing a lattice atom in the nth collision that have (1) a vacancy in their first coordination shell produced by process γ; (2) a vacancy in their first coordination shell produced by process δ; (3) an interstitial atom in the neighborhood (first to third shell, process ζ).

and because of the order in these alloys, the average concentration of aluminum atoms in the first coordination shell ($C_{Al}{}^1$) is larger than the bulk aluminum concentration C_{Al}, whereas the concentration in the second shell $C_{Al}{}^2$ is smaller than the bulk value. Replacements

TABLE III. Results of the model calculations for iron and iron-aluminum alloys with bulk aluminum concentration C_{Al}. We list the total probability for replacements R_t and the probability for direct replacements R_d. Total replacement probabilities are differentiated by sublattices (R_A, R_B, etc.). V_j is the probability for a vacancy in the jth coordination shell. I_K is the probability for a K-type interstitial atom near the replacement site. R_N is the probability for a replacement event in the neighborhood of the recoil atom. $C_{Al}{}^j$ is the average aluminum concentration in the jth coordination shell of the replacement site.

Structure	Fe	Fe_3Al		FeAl	
C_{Al}	0	0.2675	0.35	0.45	0.483
R_t	0.82	0.80	0.80	0.80	0.79
R_d	0.66	0.62	0.61	0.60	0.59
R_A	···	0.44	0.45	0.46	0.47
$R_{B'}$	···	0.15	···	···	···
R_B	···	···	0.35	0.33	0.32
$R_{B''}$	···	0.21	···	···	···
V_1	0.25	0.23	0.23	0.22	0.22
V_2	0.13	0.12	0.12	0.11	0.11
I_{Fe}	0.07	0.06	0.05	0.05	0.04
I_{Al}	···	0.02	0.03	0.04	0.04
R_N	···	0.04	0.04	0.05	0.05
$C_{Al}{}^1$	···	0.28	0.38	0.51	0.55
$C_{Al}{}^2$	···	0.27	0.30	0.36	0.38

in the neighborhood which change the atomic distribution there are rare events.

We conclude this section with a qualitative discussion of the changes of these results to be expected from a more sophisticated model of the collision process. Dederichs *et al.*[7] have shown that the probability of direct replacements is not greatly affected by the choice of the interaction potential, and also the inclusion of energy losses to the lattice does not strongly alter the occurrence of direct replacements. The local processes that we have investigated in this paper are presumably more sensitive to the model applied. In particular, we expect energy losses to the lattice to modify the result. Those processes which require low energies for both atoms after the collision, that is, local stopping collisions which lead to indirect replacements and to interstitials near the recoil atom, will be favored by the energy loss. Thus the inclusion of energy losses should bring a better agreement with the results of Refs. 5 and 6 that nearly 100% of the primary recoil atoms come to rest at lattice sites. The probability of local-vacancy production is presumably reduced by energy losses as this process requires large kinetic energies after the collision.

The model presented here is limited to binary collision processes. The energy given to the lattice could induce atoms to exchange sites, thus producing local disorder. However, the calculations by Erginsoy *et al.*[2,5,6] accounted for the motions of all atoms in small model crystallites, and did not show effects of this type. Atomic replacements occurred either as isolated events or in the form of collision sequences along close-packed crystallographic directions. Only the first two collisions of such a sequence would occur in that region near the recoil atom considered in our calculations. Within our model they are not distinguished from the double-replacement process ζ. The focusing action of surrounding atoms could result in a more frequent occurrence of this process.

4. Influence of Point Defects on ^{57}Fe Hyperfine Interactions

The combination of the experimental results and our model calculations can at the present stage lead to qualitative estimates of the effect of vacancies and interstitials on the hyperfine spectrum of ^{57}Fe recoil atoms. Apart from the simplifications used in the model, the large number of parameters associated with the possible configurations—recoil atoms in an interstitial site, interstitials and vacancies at various distances from the recoil atom—prevents a quantitative determination of the influence of these defects on the hyperfine interactions. Refinements of the model and additional experimental data will be needed to derive quantitative results.

The average shifts and magnetic fields derived from the Mössbauer spectra (Sec. II 4) suggest a net reduction of the magnetic field due to defects, beyond that caused by aluminum neighbors, and an isomer-shift contribution by defects which is smaller than that due to an aluminum neighbor, possibly of opposite sign.

The model calculations predict a preferred occupation of iron sites with a larger than bulk aluminum concentration in the first neighborhood shell. In this case the net isomer shift caused by defects must be negative. The calculated aluminum concentration in the first two coordination shells in Fe_3Al is not sufficient to explain the small average magnetic splitting observed.

We characterize the defect influences on the hyperfine interactions by the change in ground-state splitting per defect, Δg_{def}, and by the isomer-shift contribution per defect, S_{def}, similar to the effects of aluminum neighbors. There are many parameters of this kind, one for each type of defect (various interstitial sites, vacancies and interstitials in the neighborhood of a lattice site), but we have only few experimental parameters. Therefore we have used some simplifying assumptions to reduce the number of unknown parameters. First, we neglect the effect of iron interstitials near a lattice site, that is, $\Delta g_{Fe,I}=S_{Fe,I}=0$. Aluminum interstitials in the neighborhood of an ^{57}Fe atom are assumed to have an effect equal to the average effect of aluminum neighbors on lattice sites in the first and second coordination shell: $\Delta g_{Al,I}=\frac{1}{2}(\Delta g_1+\Delta g_2)=-0.15$ mm/sec, $S_{Al,I}=\frac{1}{2}(S_1+S_2)=+0.03$ mm/sec. We also assume that there is only one type of interstitial site occupied by ^{57}Fe atoms, with parameters Δg_I, S_I. Finally, the

TABLE IV. Ground-state splitting $\bar{g}$ and shift $\bar{S}$ of ^{57}Fe recoil nuclei in pure iron at 80°K.

	Calculated	Experimental
$\bar{g}$(mm/sec)	3.50	4.04 ±0.04
$\bar{S}$(mm/sec)	−0.01	−0.005±0.005.

influence of vacancies in the neighborhood of an ^{57}Fe atom is neglected beyond the first coordination shell. Vacancies in the first shell are characterized by the parameters Δg_V, S_V.

We have now estimated the influence of these defects on the magnetic hyperfine interactions (Δg_I,Δg_V) by comparing the average ground-state splitting $\bar{g}$, and the second moment $M_2^{(g)}$ derived from the fit of six Lorentz lines to the (n,γ) Mössbauer spectrum obtained in Fe_3Al at 82°K (Table I) with the corresponding values deduced from the distribution of final sites obtained in the model calculations. From this comparison we derive $\Delta g_I=\Delta g_V=-0.65$ mm/sec.

The Fe_3Al spectrum gave no good criterion for the isomer shifts. Assuming that our calculation underestimates the number of replacements at lattice sites, we have assumed zero shift for ^{57}Fe atoms at interstitial sites, $S_I=0$, and have estimated the shift due to a vacancy in the first coordination shell of a lattice site by comparing the model result with the experimental shift in FeAl with 48.3 at.% Al. This gives $S_V=-0.03$ mm/sec.

The spectrum calculated with these parameters and weights equal to the probabilities of the various configurations as given by the model results for Fe_3Al is shown in Fig. 4(b) superimposed on the experimental data. The total absorption intensity A and the widths of the individual lines γ (assumed to be the same for all lines) have been adapted so as to give minimum deviation from the data points. The values for the curve shown in Fig. 4(b) are $A=0.24$, $\gamma=0.63$ mm/sec.

The average isomer shifts of ^{57}Fe recoil atoms in FeAl structure alloys with 35 and 45 at.% Al were calculated on the basis of the model results for the final positions with the defect shifts given above and the shifts due to aluminum neighbors derived from the absorption spectra (Sec. II 2). The points obtained are interpolated by the straight line (2) shown in Fig. 2.

Finally, the average ground-state splitting $\bar{g}$ and shift $\bar{S}$ to be expected for (n,γ) Mössbauer spectra in pure iron according to our model results for the final positions of ^{57}Fe recoil atoms and with the given defect parameters can be compared with the experimental results obtained at 80°K[14,16].

In Table IV, the calculated and experimental values of the shifts agree very well. The discrepancy between the values for the ground-state splitting is substantially larger than the experimental uncertainty. This fact underlines our statement of caution regarding the qualitative character of the estimated defect influences at the beginning of this section.

ACKNOWLEDGMENTS

Felix E. Obenshain (Oak Ridge National Laboratory, guest scientist in Karlsruhe) initiated the (n,γ) Mössbauer experiments with ^{57}Fe in Karlsruhe. His encouragement and critical advice helped the promotion both of the experiments and of the efforts to trace the fate of ^{57}Fe recoil atoms. Critical discussions with Jörg Fink and Wolfgang Gläser were clarifying on many aspects of the work. One of the authors (GC) wants to acknowledge support of the U. S. Atomic Energy Commission during the stay in Karlsruhe, and he thanks Karl Heinz Beckurts and all members of the Institut für Angewandte Kernphysik for the hospitable acceptance in the Institute's stimulating atmosphere.

APPENDIX A: APPROXIMATE FIT OF UNRESOLVED SPECTRUM WITH SINGLE LINE OF LORENTZ SHAPE

Frequently an unresolved spectrum is fitted with a single line if the information available is not sufficient for a complete fit of the individual lines composing the spectrum. Conclusions about the distribution of lines can be drawn from the fitted line intensity I, position A, and width Γ. In this Appendix, we want to establish quantitatively the connection between these parameters and the moments of the distribution of lines in the spectrum.

Let us assume that n superimposed lines of Lorentz shape form the spectrum

$$M(x)=I_0\sum_{k=1}^{n}\frac{w_k}{4(x-a_k)^2/\gamma^2+1}. \tag{A1}$$

The weights w_k are assumed to be normalized,

$$\sum_{k=1}^{n} w_k=1.$$

In the data processing we find a least-squares fit to a discrete set of points. The mathematical evaluation is easier if we approximate this procedure by minimizing the integral

$$\int_{-\infty}^{\infty}\left(I_0\sum_{k=1}^{n}\frac{w_k}{4(x-a_k)^2/\gamma^2+1}-\frac{I}{4(x-A)^2/\Gamma^2+1}\right)^2 dx. \tag{A2}$$

Differentiation with respect to I, A, and Γ, and integration over x leads to the equations

$$\begin{aligned}
&\sum_{k=1}^{n}\frac{w_k}{4(A-a_k)^2/(\Gamma+\gamma)^2+1}=\frac{I(\Gamma+\gamma)}{2I_0\gamma},\\
&\sum_{k=1}^{n}\frac{w_k(A-a_k)}{[4(A-a_k)^2/(\Gamma+\gamma)^2+1]^2}=0,\\
&\sum_{k=1}^{n}\frac{w_k(A-a_k)}{[4(A-a_k)^2/(\Gamma+\gamma)^2+1]^2}=\frac{I(\Gamma+\gamma)^3(\Gamma-\gamma)}{32I_0\Gamma\gamma}.
\end{aligned} \tag{A3}$$

We can expand the denominators on the left-hand sides of Eqs. (A3) if we can assume that $|A-a_k|$

$<\frac{1}{2}(\Gamma+\gamma)$ for all k. This condition might seem very restrictive, but it is just the quantitative expression of the assumption that the spectrum is unresolved. Any line for which the condition is not fulfilled will be clearly separated from the other lines and should not be included in the single-line fit. We carry out the expansion and introduce the moments

$$\langle a\rangle=\sum_{k=1}^{n} w_k a_k, \qquad M_l=\sum_{k=1}^{n} w_k(a_k-\langle a\rangle)^l.$$

The final result is then expressed as a series in terms of order M_l/Γ^l:

$$\gamma^2=\Gamma^2-8M_2+8\frac{2M_4-3M_2^2}{\Gamma^2}+\cdots, \tag{A4}$$

$$A=\langle a\rangle-2\frac{M_3}{\Gamma^2}+\frac{3M_5-20M_2M_3}{\Gamma^4}+\cdots, \tag{A5}$$

$$\frac{I}{I_0}=1-3\frac{M_2}{\Gamma^2}+\frac{5M_4-16M_2^2}{\Gamma^4}+\cdots. \tag{A6}$$

APPENDIX B: SELF-ABSORPTION IN FeAl STRUCTURE ALLOY TARGETS

Self-absorption in Mössbauer sources containing resonantly absorbing nuclei diminishes, in general, the recoilless fraction of the γ rays leaving the source and broadens the emitted line.[31] In our FeAl-structure alloy targets, prepared with natural iron containing 2.2% ^{57}Fe, the γ rays are emitted by nuclei in an environment which differs from that of the lattice atoms, as evidenced by the observed shifts of the Mössbauer spectra. The resonant self-absorption is centered at an energy which differs from the average energy of the recoil-free emitted γ rays. Consequently, self-absorption in these targets is asymmetric with respect to the emitted line and introduces an additional shift of the line. We estimate this shift assuming Lorentzian emission and absorption lines centered at energies x_0 and x_1, respectively. Broadening in the alloys due to variations in the neighborhood are taken into account by the introduction of effective widths Γ_0 of the emission line, and Γ_1 of the absorption cross section. The energy spectrum of the recoil-free γ rays leaving the target is proportional to

$$I_d(x)=\frac{1}{(x-x_0)^2+a^2}\frac{(x-x_1)^2+b^2}{(x-x_1)^2+c^2}\times\left\{1-\exp\left[-\left(\frac{b^3\beta f\sigma_0}{(x-x_1)^2+b^2}+\bar{\sigma}\right)nd\right]\right\}. \tag{B1}$$

The meanings of the as yet undefined symbols are $\sigma_0=2\times10^{-18}$ cm^2, the maximum cross section for resonance absorption; $\bar{\sigma}=0.9\times10^{-20}$ cm^2, the cross section for electronic absorption; $\beta=0.022$, the isotopic concentration of ^{57}Fe; f is the recoilless fraction for absorbing nuclei; n is the number of iron atoms per cm^3; d is the target thickness (in cm); $a=\frac{1}{2}\Gamma_0$; $b=\frac{1}{2}\Gamma_1$; $c=b(1+\beta f\sigma_0/\bar{\sigma})^{1/2}$. The numerical values inserted are appropriate for the 14.4-keV γ rays of ^{57}Fe. Electronic absorption by aluminum in the alloys can be neglected.

The exponential term contains the constant factor $\exp(-\bar{\sigma}nd)\sim0.1$ for our targets. The contribution of this term is less than 10% of the self-absorption shift, and we neglect it. This is equivalent to the thick-source approximation ($d\to\infty$).

We have shown in Appendix A that a set of closely spaced Lorentzian lines can be approximated by a single line of Lorentz shape whose center is in first approximation located at the average $\langle a\rangle$ of the positions of the individual lines. We assume that in the present case the apparent line center is approximately given by the first moment of $I(x)$:

$$\langle x\rangle=\mathcal{P}\int_{-\infty}^{\infty} xI_\infty(x)dx \Big/ \int_{-\infty}^{\infty} I_\infty(x)dx. \tag{B2}$$

In the numerator we have to evaluate the principal value. Otherwise the integral is not defined.

We substitute (B1) with $d\to\infty$ into (B2) and obtain the result

$$\langle x\rangle=x_0+\frac{ab^2\beta f\sigma_0(x_0-x_1)}{\bar{\sigma}[c(x_0-x_1)^2+(b^2+ac)(a+c)]}. \tag{B3}$$

All quantities in this equation except the center of the emission line x_0 are known or can be derived from the target and absorption spectra obtained with the alloys.

TABLE V. Line shifts due to self-absorption in FeAl structure targets. The meaning of the symbols is explained in the text.

C_{Al}	T (°K)	f	a (mm/sec)	b (mm/sec)	c (mm/sec)	x_1 (mm/sec)	$\langle x\rangle$ (mm/sec)	x_0 (mm/sec)
0.35	298	0.7	0.2	0.1	0.21	0.158	0.084	0.101
0.45	298	0.7	0.2	0.1	0.21	0.231	0.096	0.126
0.483	82	0.9	0.2	0.05	0.12	0.248	0.110	0.136
0.483	298	0.7	0.2	0.05	0.11	0.255	0.116	0.139
0.483	573	0.45	0.2	0.05	0.09	0.256	0.137	0.153
0.483	773	0.3	0.2	0.05	0.08	0.257	0.143	0.156
0.515	298	0.7	0.2	0.05	0.11	0.276	0.122	0.147

In Table V we summarize the relevant parameters, the observed shifts $\langle x \rangle$ and the calculated shifts x_0 of the emission ines for our alloy targets with FeAl structure.

We have not corrected the spectra obtained with the Fe_3Al target for self-absorption. There, too, the centers of emission lines and of self-absorption cross sections do not coincide. But the effects of self-absorption are greatly diminished by the magnetic splitting. The maximum cross section is only about $\frac{1}{6}$ of that in paramagnetic FeAl structure targets, and the shifts due to self-absorption do not exceed the experimental uncertainty of the line centers.

PHYSICAL REVIEW B VOLUME 1, NUMBER 3 1 FEBRUARY 1970

Low-Temperature Pressure-Dependence Studies of Knight Shifts and Nuclear Spin-Lattice Relaxation Rates in Cesium and Rubidium Metals*

H. T. WEAVER AND ALBERT NARATH
Sandia Laboratories, Albuquerque, New Mexico 87115
(Received 8 July 1969)

Measurements of the Knight shift K and nuclear spin-lattice relaxation-time T_1 have been carried out on ^{133}Cs and ^{87}Rb as a function of hydrostatic pressure to 50 000 psi at 4°K. For ^{133}Cs, atmospheric-pressure data were also obtained at 27 and 76°K. The cesium Knight shift and relaxation rate are enhanced by about 18 and 24%, respectively, at the maximum pressure. This corresponds to a 13% increase in the Korringa product K^2T_1T, which is attributed to an increase in the exchange enhancement of the spin susceptibility resulting from a strong volume dependence of the band effective mass. The experimental volume and temperature derivatives of K in cesium metal yield an explicit temperature dependence at 4°K given by $(\partial \ln K/\partial T)_V = -(0.8\pm0.1)\times10^{-4}°K^{-1}$.

I. INTRODUCTION

THE spin susceptibilities χ of the alkali metals are enhanced significantly relative to the independent-particle susceptibilities $\chi_0=\chi_P m_0^*/m_0$ (where χ_P is the Pauli free-electron susceptibility, and m_0^*/m_0 is the band effective mass ratio) by collective-electron effects. This has been demonstrated by a variety of experimental techniques. The early measurements of the lithium susceptibility by Schumacher and Slichter,[1] and that of sodium by Schumacher and Vehse,[2] were based on determinations of the absolute areas under the conduction-electron spin-resonance absorption curves. Ryter[3,4] subsequently obtained essentially identical values for these susceptibilities from measurements of hyperfine-induced g shifts of the conduction-electron resonances. Estimates for the alkali-metal spin susceptibilities have also been obtained by Kaeck,[5] who inferred the dependence of χ on atomic volume from the systematic variation of the alkali Knight shifts in liquid binary alloys. The enhancement factors have been determined more directly by Schultz and Dunifer[6] for sodium, potassium, rubidium, and cesium from observations of spin-wave sidebands in the transmission conduction-electron spin-resonance spectra. An interesting feature of the available experimental results is the relatively weak dependence of the collective-electron enhancement on atomic volume. Whereas the latter increases by a factor of 2.8 in the sequence sodium to cesium, the ratio χ/χ_P increases by a factor of only $\sim$1.3. Moreover, it is likely that a significant fraction of the observed increase in χ/χ_P simply reflects a band-structure enhancement of the independent-particle susceptibility χ_0 of cesium and to a lesser extent that of rubidium. It is noteworthy that a recent calculation by Rice[7] yielded nearly identical χ/χ_P ratios for sodium and potassium, in good agreement with experiment.

That the enhancement of the alkali-metal spin susceptibilities due to electron-electron interactions is nearly constant has also been inferred recently from measurements[8] of the nuclear magnetic resonance (NMR) shifts K and spin-lattice relaxation rates T_1^{-1}. The experimental Korringa products K^2T_1T were shown to exceed the independent-particle prediction $\mathcal{S}$ by approximately 60% in all five alkali metals. In nearly free-electron metals, and in the absence of non-s hyperfine interactions, the ratio $K^2T_1T/\mathcal{S}$ depends only on the electron-electron interaction. A convenient measure of the strength of this interaction is the Stoner enhance-

* This work was supported by the U. S. Atomic Energy Commission.

[1] R. T. Schumacher and C. P. Slichter, Phys. Rev. **101**, 58 (1956).

[2] R. T. Schumacher and W. E. Vehse, J. Phys. Chem. Solids **24**, 297 (1963).

[3] C. Ryter, Phys. Rev. Letters **5**, 10 (1960).

[4] C. Ryter, Phys. Letters **5**, 69 (1963).

[5] J. A. Kaeck, Phys. Rev. **175**, 897 (1968).

[6] S. Schultz and G. Dunifer, Phys. Rev. Letters **18**, 283 (1967); and private communication. The susceptibilities are obtained by combining the spin-wave data with the effective masses given by C. C. Grimes and A. F. Kip, Phys. Rev. **132**, 1991 (1963); C. C. Grimes, G. Adams, and P. H. Schmidt, Bull. Am. Phys. Soc. **12**, 414 (1967).

[7] T. M. Rice, Phys. Rev. **175**, 858 (1968).

[8] A. Narath and H. T. Weaver, Phys. Rev. **175**, 373 (1968).